DMD2018-6834

FRACTURE TOUGHNESS CHARACTERIZATION AND MIXED-MODE FRACTURE FINITE ELEMENT MODELING FOR ACCURATE BIOPSY NEEDLE CUTTING FORCE PREDICTION

Ng Si Yen
National Cheng Kung University
Tainan City, Taiwan (R.O.C)

Guan-Jhong Lan
National Cheng Kung University
Tainan City, Taiwan (R.O.C)

Chi-Lun Lin
National Cheng Kung University
Tainan City, Taiwan (R.O.C)

BACKGROUND

Fracture toughness is an important mechanical property of materials that describes the failure of material by cracking. Yet, characterizing fracture toughness in soft tissue cutting is still a challenging task as the behavior of the soft tissue may vary under different tissue, cutting and pre-crack conditions [1]. Predicting cutting force has been important to needle biopsy design, surgical planning/training, and other surgical operations. However, in order to obtain accurate predictions, understanding the fracture toughness is crucial. In this study, we present an approach to characterize the fracture toughness directly from cutting experiments of hollow needle cutting soft tissue mimicking materials. Cutting tests are carried out to obtain the dynamic force response of gelatin samples when being cut by non-rotational and rotational hollow needles. The data is used to establish a mixed-mode fracture behavior which is then used to implement a cohesive surface based finite element model. Nearly 1% difference of the axial cutting force between the simulation and experimental results showed that the approach is capable of predicting accurate cutting force in rotational needle biopsy. The approach also has the potential to be used to predict the cutting force in various types of needle biopsy.

METHODS

Samples of gelatin tissue phantom (wt. 16.6 %) were fabricated and tested to characterize their mechanical behavior when experiencing deformation and fracture. The indentation test was first conducted using MTS INSIGHT-1 to obtain the relationship between the compressive force and displacement, which was then used to fit into a Yeoh hyperelastic material model, as shown in Table 1. Next, samples made with the same procedure were tested in a cutting platform (Fig. 1), on which a hollow needle was driven by a linear and a rotary motor to perform cutting tasks with different cutting speeds. The HBM-S2M force transducer was used for the measurement of the axial tissue reaction force during the cutting process. The outer diameter of the needle was 3.4 mm and the inner diameter was 2.6 mm, with a circular incision of angle 12° at the tip. The size of the tissue phantom samples was 50mm (length)×50mm (width)×25mm (thickness) and was placed in an acrylic container with a circular window facing the needle for it to pass through. The opposite side of the container was open to allow the tissue to full contact a metal plate, which was connected to the force transducer, for measuring the tissue reaction force during the cutting process.
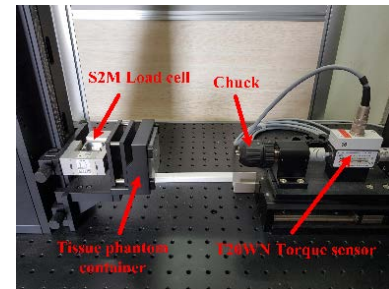

Figure 1: Needle cutting platform.

Table 1: Yeoh hyperelastic material model parameters.

D_1	D_2	D_3	C_{10}	C_{20}	C_{30}
3.1081	0	0	3.2282E-3	-1.5056E-3	5.7006E-4

In the cutting test, a gelatin sample was cut by the needle twice. The first insertion was performed on an intact sample to measure force response of a regular cutting process. The second insertion was through the cutting path produced by the first one to measure mainly the friction force between the sample material and the needle. The fracture toughness was calculated through the theoretical formula [2] as Eqn. 1,

$$J = \frac{\int (F_1 - F_2) du}{\int dA} \quad (1)$$

where J is the fracture toughness of the material, F1 and F2 were the force responses in the cutting phases during first and second insertions, respectively, u was the displacement of the needle, and A was the fracture area produced during the first needle insertion, i.e. the product of the inner circumference of the needle and the cutting depth, as shown in Fig. 2.
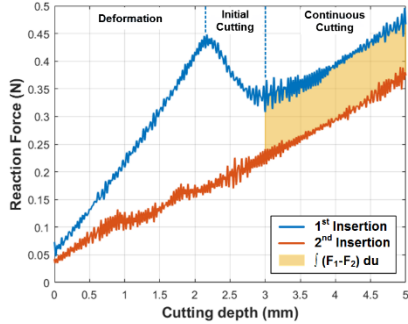

Figure 2: Region selection for fracture toughness calculation.

For non-rotational needle cutting, the cutting test was carried out with four different needle translation speeds (2, 5, 8, 12 mm/s) to measure the fracture toughness. To investigate the effect of the needle rotation on the fracture toughness, three different slice push ratios (0.5, 1, 3) at the needle translation speed of 2 mm/s were also tested. For each cutting speed configuration, including rotational and non-rotational cutting cases, six times of the cutting test were conducted. In addition, the sequences of the tests were randomly assigned. ABAQUS 6.14 was used to establish a finite element model (Fig. 3), simulate the process of rotational and non-rotational cases, and analyze its mechanical effects under different cutting speeds and slice push ratios. The gelatin tissue phantom was assigned as a hyperelastic material with a density of 1480 kg/m3 and Poisson's ratio of 0.495. In this model, general contact properties were used and all contact surfaces between elements will follow the Coulomb's friction law. The static friction coefficient, μ_s was 0.6 and the dynamic friction coefficient, μ_k was 0.3. The cohesive surface was arranged on both sides of a predefined crack path, which was a thin, cylindrical surface along the axial direction of the needle (Fig. 4). To ensure the needle would pass through the predefined crack path, a custom constraint was added to dynamically check the radial displacement of each cohesive node in each time increment. When the cohesive node was displaced from the predetermined crack path, it would be slightly adjusted back to the path.
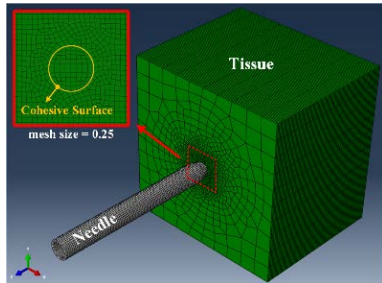

Figure 3: A three-dimensional finite element model for the cutting process.
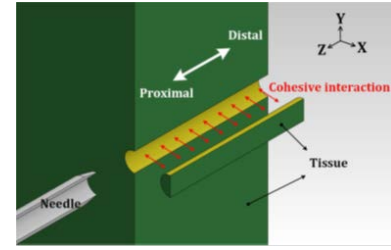

Figure 4: The finite element model (cross-sectional view) and the arrangement of the cohesive surface.

In order to simulate the three-dimensional fracture, a mixed mode response for the cohesive surface, including Mode I (opening), Mode II (sliding shear) and Mode III (tearing shear), were determined. We assumed that the total fracture toughness (the sum of the three modes) of the gelatin samples was constant at a certain needle insertion speed. When the needle rotation was involved, the fracture toughness of Mode I would reduce and the reduced portion would be instead contributed by the shear Modes. Therefore, by comparing the fracture toughness obtained from the non-rotational and rotational cutting cases, proportions of threes fracture modes were identified. Since the needle had a thin circular cutting tip surface and was constrained to pass through the pre-defined crack path where the cohesive surface was arranged, we hypothesized that the Mode II would be the most unlikely to occur during the cutting simulation, thus it was assumed no contribution to the total fracture toughness.

To obtain the traction-separation relationship from the measured fracture toughness, two additional assumptions were made: (a) shear force is more likely to cause the fracture to the soft tissue phantom than the normal force [3]. Therefore, the stiffness factor of Mode III should be smaller than the value given in Mode I; (b) the ratio of the separation at the damage initiation and the end of the damage evolution is 0.9 in each mode [4].

In order to validate the FE model, the simulation results were compared with the experimental results of non-rotational (2 mm/s) and rotational cutting (SPR = 1) cases.

RESULTS

The results of the fracture toughness obtained under different speeds of non-rotational cutting cases were plotted as shown in Fig. 5. The fracture toughness had a nearly linear growth with the increase of the needle insertion speed in the range between 2 and 8 mm/s. However, there was a significant reduction of the fracture toughness when the needle insertion speed increased from 8 to 12 mm/s.

The experimental results for the fracture toughness obtained under different slice push ratios with needle insertion speed at 2 mm/s were plotted as shown in Fig. 6. Initially, the fracture toughness increased rapidly with the increase of slice push ratio, but started to decrease slowly after the slice push ratio reached 0.5.
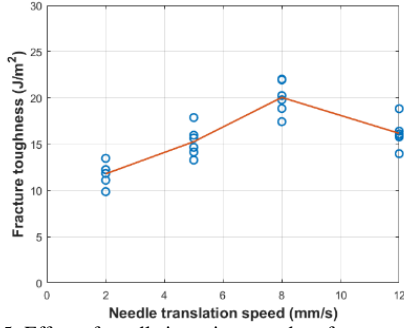
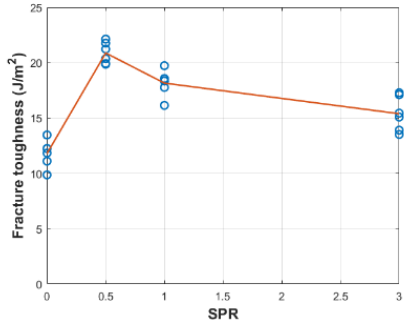Figure 5: Effect of needle insertion speed on fracture toughness.

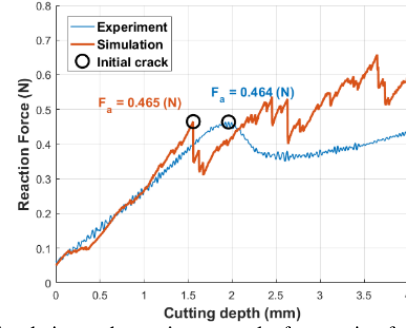Figure 6: Effect of slice push ratio on fracture toughness.

Figure 7: Simulation and experiment results for reaction force on needle tip (Non-rotational cutting).
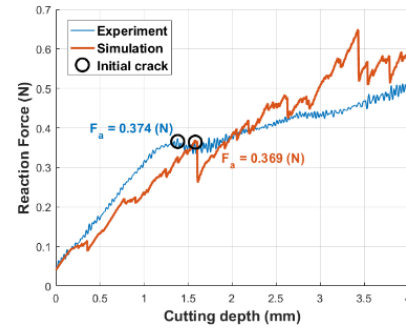
Figure 8: Simulation and experiment results for reaction force on needle tip (Rotational cutting).

The total fracture toughness (the sum of the three fracture modes) was calculated under different needle insertion speeds. From the reduction of the cutting force measured in the rotational cutting cases at the needle insertion speed of 2 mm/s, we estimated the ratio of the fracture toughness in the shear mode. Therefore, the parameters for both normal and shear fracture modes were obtained for the finite element model, as shown in Table 2 and 3, respectively.

The comparisons of the experimental and simulation results were shown in Fig. 7 and Fig. 8. For the non-rotational case, the initial crack point from simulation was at the depth of 1.559 mm and it was at the depth of 1.960 mm observed from the experimental result. The cutting force obtained from the simulation was 0.465 and 0.369 N for the non-rotational and rotational cases, which had percentages of error of 0.216% and 1.337% compared to the experimental results (0.464 and 0.374 N).

Table 2: Cohesive parameters (Needle insertion speed=2 mm/s, SPR=0)

	$G_C(J/m^2)$	Mixed mode ratio	t_c(MPa)	K(N/mm³)
Normal	11.7916	1	0.5	11.7925
Shear		0	N.A.	N.A.

Table 3: Cohesive parameters (Needle insertion speed=2 mm/s, SPR=1)

	$G_C(J/m^2)$	Mixed mode ratio	t_c(MPa)	K(N/mm³)
Normal	18.1530	0.6496	0.5	11.7925
Shear		0.3504	0.25	5.4583

INTERPRETATION

Observing from the cases of non-rotational needle cutting, the fracture toughness of gelatin increased linearly with the increase of the needle insertion speed but it dropped sharply after the needle insertion speed was higher than 8mm/s. We speculated that in the lower needle insertion speed range, the fracture was caused mainly by axial compression. When the needle insertion speed reached a certain value, which was 8 mm/s in this case, the momentum of needle increased much so that it resulted in the reduction of the fracture toughness. More experiments need to be conducted to locate the exact threshold of the needle insertion speed and identify the root cause to this phenomenon.

From the relationship between fracture toughness and slice push ratio as shown in Fig. 6, the fracture toughness of Mode I for gelatin samples under different slice push ratios can be assumed as the total fracture toughness obtained in the non-rotational needle cutting. In other words, fracture ratio in shear mode increased drastically with the increase in slice push ratio. However, this effect gradually declined with the increase in slice push ratio after it reached 0.5. Therefore, the slice push ratio of 0.5 can efficiently produce the tangential needle force to cause the crack.

The axial cutting force of the needle can be predicted accurately through our cohesive surface based finite element model. Percentage of error for simulated axial cutting force in the non-rotational and rotational cutting cases, compared with experiments, were only 0.216% and 1.337% respectively. However, the predicted initial crack points by the finite element model was earlier than the experimental results by about 0.4 mm

for non-rotational case and was later than the experimental results by about 0.2 mm for rotational case. This was caused by the assumptions made for the stiffness K in the traction-separation relationships. If K was assumed smaller than the realistic value, the gradient of the initial rising slope was smaller such that the initial crack point was predicted later than the experimental results. Further experiments need to be designed and performed to identify this parameter in order to obtain a more accurate prediction of the initial crack. However, in terms of predicting the axial cutting force, the accuracy of the presented finite element model was reliable.

ACKNOWLEDGMENTS

REFERENCES

[1] Taylor, D., O'Mara, N., Ryan, E., Takaza, M., and Simms, C., 2012, "The Fracture Toughness of Soft Tissues," J. Mech. Behav. Biomed. Mater., 6(C), pp. 139–147.

[2] Gokgol, C., Basdogan, C., and Canadinc, D., 2012, "Estimation of Fracture Toughness of Liver Tissue: Experiments and Validation," Med. Eng. Phys., 34(7), pp. 882–891.

[3] Atkins, A. G., Xu, X., and Jeronimidis, G., 2004, "Cutting, by 'Pressing and Slicing,' of Thin Floppy Slices of Materials Illustrated by Experiments on Cheddar Cheese and Salami," J. Mater. Sci., 39(8), pp. 2761–2766.

[4] Oldfield, M., Dini, D., Giordano, G., and Rodriguez y Baena, F., 2013, "Detailed Finite Element Modelling of Deep Needle Insertions into a Soft Tissue Phantom Using a Cohesive Approach," Comput. Methods Biomech. Biomed. Engin., 16(5), pp. 530–543.